LAWRENCE
LIVERMORE
NATIONAL
LABORATORY

LLNL-JRNL-529853

Simulating the MAGLIF Plasma Confinement with Smaller-Scale Experiments

D. D. Ryutov, M. C. Herrmann, S. A. Slutz

February 16, 2012

The Physics of Plasmas

Disclaimer

LLNL-JRNL-529853

Simulating the MagLIF plasma confinement with smaller-scale experiments

D.D. Ryutov[1], M.E. Cuneo[2], M.C. Herrmann[2], D.B. Sinars[2], S.A. Slutz[2]

[1] *Lawrence Livermore National Laboratory, Livermore, CA 94551*
[2]*Sandia National Laboratories, Albuquerque, NM, 87185*

Abstract

The recently proposed MagLIF approach to a Z-pinch driven fusion [S.A. Slutz et al., Phys. Plasmas, **17**, 05603 (2010)] relies on suppression of the plasma heat flux to the walls of the imploding liner by magnetizing the plasma. The characteristic plasma transport regimes in the proposed approach cover parameter domains that have not been studied yet in either magnetic confinement or inertial confinement experiments. In this article, an analysis is presented of the scalability of the key physical processes that determine the plasma confinement. The dimensionless scaling parameters are identified and conclusion is drawn that the plasma behavior in scaled-down experiments can correctly represent the full-scale plasma, provided these parameters are approximately the same in two systems. This observation is important in that smaller-scale experiments typically have better diagnostic access and more experiments per year are possible.

I. INTRODUCTION

The recently proposed MagLIF concept is based on compressing magnetized fusion fuel plasma using a current-driven cylindrical liner implosion [1]. The magnetized fuel density in MagLIF will be much higher than in typical experiments on magnetic confinement fusion [2] and it will be much lower than in laser-driven inertial confinement fusion experiments [3]. Accordingly, characteristic time-scales will lie in between the time-scales typical for magnetic confinement fusion, which are, roughly, 1-10 seconds, and those typical for inertial confinement fusion, which are $\sim 10^{-9}$ s. The plasma in the MagLIF approach will be imploded at the velocity much smaller than the plasma sound velocity and will therefore pass through a sequence of radial equilibria supported by the heavy liner. In order to maintain the heat loss to the liner surface at an acceptable level, one would use the axial magnetic field, which would suppress the heat conduction to the liner-plasma interface. The heat loss to the ends remains uninhibited, but can be made tolerable by using sufficiently long liners. For realistic lengths, the implosion time would have to be in the range of ~100 ns, which is achievable with the drivers of the scale of a Z facility at Sandia [4]. In this regard, the MagLIF concept is different from several other approaches to the liner-compressed plasma, which use slower liners and therefore have to rely on a 3-dimensional plasma thermal insulation from the cold liner (e.g. Refs. [5-8] and references therein).

The plasma behavior in the imploding liner is one of the factors defining the success or failure of the MagLIF approach. On the other hand, systematic studies of the plasma confinement in a full-scale MagLIF experiments will be hindered by the

difficulties of the diagnostic access and relatively low shot rate. It is therefore important to identify conditions, under which certain aspects of an overall confinement problem could be studied at smaller-scale facilities. Of course, there is no way to produce the same (as in MagLIF) plasma at these smaller-scale facilities, but one can hope that, by identifying the proper scaling parameters, one would be able to find conditions where these smaller-scale experiments would be able to properly assess at least some sub-sets of controlling phenomena. This scaling study is the main goal of our paper. For other examples of scalings for time-evolving high-energy-density plasmas see Refs. 9, 10 and references therein.

In the course of one implosion, the plasma passes through a sequence of different confinement regimes. Reproducing a complete sequence of these regimes in one scaled-down experiment is hardly possible, as they are very different in the sense of governing parameters, and we suggest a different approach, where scaled-down experiments would imitate the plasma confinement at limited segments of the implosion process. Then, the set of such experiments would cover the whole implosion process.

In the current-driven liner implosions, the plasma pressure is typically less than the external magnetic field pressure until the time immediately preceding the stagnation point: at this last segment the plasma pressure rapidly reaches the values exceeding the external pressure and the liner slows down and rebounds. A very convenient analytical expression for the 1D liner trajectory has been suggested in Ref. 11 for a power-law time dependence of the implosion current. This expression is quite useful for the general assessment of the desirable parameters of the liner and the current drive.

The overall success of the MagLIF concept depends not only on the plasma performance but also on the quality of the liner implosion, in particular the liner stability. We, however, do not consider this part of the problem, assuming that the liner behaves well-enough. The encouraging experimental results on the liner stability are presented in Refs. 12, 13.

If the liner performs as anticipated, it can be considered as a slowly moving (slowly compared to the plasma sound speed) external wall compressing the plasma, see below. So, the possible faster plasma instabilities, which we are concerned with in this study, would show up even if we (conceptually) freeze the liner position and then, as discussed in the previous paragraph, look at the plasma transport for this "frozen" liner configuration.

The rest of the paper is organized as follows. In Sec. II, we identify four dimensionless parameters whose constancy between two plasmas guarantees the similarity of the physical processes, up to the scale transformations of spatial coordinates and time. In Sec. III this scaling approach is used to assess the feasibility of smaller-scale experiments that would be a scaled-down analogue of the real plasma. We emphasize that our paper does not contain an answer to the question of the plasma confinement times. It just identifies the smaller-scale experiments which would provide such an answer for a full system. In Sec. IV, we consider specific examples of scaled-down experiments and in Sec. V analyze the possible further energy saving by switching from deuterium to hydrogen.

II. DIMENSIONLESS SCALING PARAMETERS

The plasma parameters in a MAGLIF implosion vary significantly during one implosion. Their typical values for a typical implosion are illustrated by Table 1 based on Ref. 1. The first line in Table 1 corresponds to the initial, pre-implosion plasma, just created inside the liner by some auxiliary power source (possibly, pulsed laser, see Ref. [1]). The second line corresponds to an intermediate stage, where the liner radius decreased by a factor of 5 compared to its initial value. The third line corresponds to the point of the maximum compression. This is some typical set of parameters, not necessarily optimized for the best performance; it just provides guidance for the scaling analysis. The parameter τ^* in the middle column represents a rough estimate of the time the system spends near the chosen point, based on the simulations of Ref. 1. The plasma confinement time must be longer than this time for the system to work. The meaning of the parameters in the right part of the table will be discussed shortly.

The plasma in MAGLIF is highly collisional: the time τ^* is much longer than the electron-ion energy exchange time $\tau_{ei}^{(E)}$, see below. For this reason, we characterize the plasma by a single temperature T. The other plasma parameters are the plasma density n, and the magnetic field strength B; the geometrical parameters are the plasma radius a and the plasma length L. So, the full set of parameters defining the initial plasma state is:

$$n, T, B, L, a. \tag{1}$$

By "dialing in" these five parameters, one defines the further evolution of the plasma, including the possible formation of a denser colder plasma in the transition zone to the colder liner. But our main concern will be the region of the hotter plasma where the appearance of an anomalous cross-field transport and strong distortion of the confining

magnetic field is a distinct possibility (e.g., [14-16]). A good confinement of the hot plasma, in the region where the temperature decreases by a factor of 5 to 10 from its maximum value on axis is a necessary condition for the MagLIF concept to work.

In a simulation experiment, by creating plasma in some initial state and then allowing it to evolve, one would obtain the information on the characteristic decay time, as well as more subtle features, such as the most prevalent instability modes (if any). The outcome of this thought experiment is entirely determined by the initial values of n, T, B, plus geometrical parameters a, and L. If the scaling parameters that we identify below are held the same between the two plasmas, their behavior will be identical, just temporal and spatial scales change.

The plasma is supposed to be an equi-component mixture of deuterium and tritium; we characterize it by the ion mass m_i equal to 2.5 proton mass m_p. For evaluating the ion thermal speed $\mathrm{v}_{Ti} = \sqrt{2T/m_i}$ and the ion gyro-radius $\rho_i = \mathrm{v}_{Ti}/\omega_{Ci}$ (with ω_{Ci} being the ion cyclotron frequency) we use the following numerical expressions:

$$\mathrm{v}_{Ti}(cm/s) \approx 3\cdot 10^7 \sqrt{T(keV)}\ ;\ \rho_i(\mu m) \approx 78\sqrt{T(keV)}/B(MG)\ . \qquad (2)$$

The electron gyro-radius ρ_e is equal to $\sqrt{\mu}\rho_i$, with $\mu = m_e/m_i = 1/4610$ .When evaluating the Coulomb mean-free-path λ, we ignore the dependence of the Coulomb logarithm on plasma parameters and use the following expression:

$$\lambda(\mu m) \approx 3\cdot 10^{22}\left[T(keV)\right]^2/n(cm^{-3})\ . \qquad (3)$$

For the general scaling analysis, where the parameters vary by several orders of magnitude, the use of these rough expressions is sufficient. Eqs. (2), (3) have been used for filling out the corresponding columns in Table 1. The plasma energy content that

enters the Table is defined as $W = \pi a^2 L \times 3nT$ (i.e., it accounts for the contributions of both electrons and ions) and is numerically evaluated as

$$W(kJ) = 1.5 \cdot 10^{-21} n(cm^{-3}) T(keV) \left[a(mm)\right]^2 L(mm) \ , \tag{4}$$

with the temperature, density, and geometrical parameters as in other rows of the Table. The electron-ion energy exchange time is defined as

$$\tau_{ei}^{(E)} = (\lambda / \sqrt{\mu} \mathrm{v}_{Ti}) \ . \tag{5}$$

It is indeed quite short compared to the anticipated confinement times, thereby justifying the use of a model with equal electron and ion temperatures.

To find the conditions under which two initial plasmas with different set of initial parameters and different a and L evolve similarly (i.e. their spatio-temporal evolution is the same up to some scaling factors), it is convenient to measure the distances in terms of a parameter a and the time in terms of the acoustic time

$$\tau = a / \mathrm{v}_{Ti}. \tag{6}$$

We introduce the following dimensionless scaling parameters:

$$R_1 = \frac{a}{\rho_i} \ ; \ R_2 = \frac{a}{\lambda} \ ; \ R_3 \equiv \beta = \frac{16\pi nT}{B^2} \ ; \ R_4 = L / a \ . \tag{7}$$

Since the number of input parameters (1) is 5, specifying the radius and 4 dimensionless parameters (7) is equivalent to specifying the 5 input parameters (1). Specifically,

$$n(cm^{-3}) = 7.6 \cdot 10^{16} \frac{\beta R_1^2}{\left[a(mm)\right]^2} ; T(keV) = \frac{0.05}{\sqrt{a(mm)}} R_1 \sqrt{\frac{\beta}{R_2}} \ ; \tag{8}$$

$$B(MG) = \frac{1.74 \cdot 10^{-2}}{\left[a(mm)\right]^{5/4}} \frac{R_1^{3/2} \beta^{1/4}}{R_2^{1/4}} ; L = R_4 a \tag{9}$$

The Jacobian of the transformation (7) from five input variables (1) to four dimensionless parameters (7) and a is expressly non-zero, $\partial(n,T,B,L,a)/\partial(R_1,R_2,R_3,R_4,a) = nTBL/2R_1R_2R_3R_4$, meaning that the dimensionless parameters are independent.

The unit of the time (6) is also uniquely defined in terms of the parameters (7) and radius a:

$$\tau(ns) = 15\left[a(mm)\right]^{5/4} \frac{R_2^{1/4}}{\beta^{1/4} R_1^{1/2}} \,. \tag{10}$$

We emphasize that τ is just a convenient unit of time, not the plasma confinement time, which has to be much longer to be of interest for MagLIF and which, as we show, can be determined from the scaled experiments.

The set of equations (7)-(9) allows one to identify all the systems that would evolve similarly to the initial one: to do that, one has to take the main dimensionless parameters the same, and vary a. [Instead of parameters (7) one could choose their various independent combinations, like, e.g., a quadruplet of parameters R_1R_2, R_1/R_2, R_3 and R_4. We have chosen parameters (7) because of their very simple physical meaning.] The plasma energy (4) can be represented as

$$W(kJ) = 5.7\cdot 10^{-6} \frac{\beta^{3/2} R_1^3 R_4}{\sqrt{R_2}} \sqrt{a(mm)} \,. \tag{11}$$

In Table 2, we present numerical values of scaling parameters corresponding to rows 1 and 2 of Table 1. It goes without saying that, if one substitutes for a the value

from Table 1, and for the dimensionless parameters their values from Table 2, one obtains for W, n, T, B and τ their values from Table 1 (up to the rounding errors).

One can see that, at the stage 1, the ions are un-magnetized in the sense that their mean-free path is much shorter than their gyro-radius, $R_2>>R_1$. The electrons, whose gyro-radii are 70 times smaller, are still magnetized. In combination with a very high plasma beta, this creates an interesting setting that has not yet been studied in any detail either theoretically or experimentally.

At the stage 2, the ions are strongly magnetized and their radial thermal conduction is strongly suppressed. On the other hand, as we will show shortly, the collision frequency still remains high compared to the drift frequency, thereby bringing this regime close to that considered theoretically in Refs. 15, 16. We are not aware of any experimental studies of the high-beta plasma transport in this regime. The parallel confinement is collisional in both cases: the mean-free path is much shorter than L.

The classical confinement, not involving development of turbulence and describable by axisymmetric two dimensional (r-z) Braginski equations [17] lead to favorable predictions with regard to the plasma states achievable in MagLIF implosions [1]. On the other end of the spectrum of confinement scenarios are those of turbulent plasma transport, in particular via the collisional drift-wave turbulence [15, 16]. As a reference value for the resulting anomalous transport coefficients, the Bohm diffusion coefficient is often used, defined as (in CGS):

$$D_B = \frac{1}{16}\frac{cT}{eB} . \qquad (12)$$

One should emphasize that the anomalous transport produced by the drift turbulence in collisionless plasma can give rise to transport coefficients exceeding Eq. (12) by an order

of magnitude and, possibly, more [14], making it hard to reach the temperatures of 5-8 keV needed for reaching the fusion breakeven. In the collisional case the predictions are much more favorable.

The mesoscale plasma turbulence in a high-beta plasma may lead also to tangling of the imposed axial magnetic field. This may increase the connection length between the center and the end surfaces, thereby significantly improving the axial confinement and (potentially) allowing to shorten the plasma length. On the other hand, the magnetic field tangling may increase the radial heat losses vial electron channel.

This brief discussion shows the richness of the physics effects that may show up in the virtually unexplored domain of plasma parameters. The focus of our paper is on finding out whether one can experimentally study the transport coefficients in the smaller, less energy-intensive experiments than a full-scale MagLIF, and still be confident that an extrapolation to MagLIF is reliable. So, we resort to the scaling analysis to find out the requirements under which these smaller experiments would correctly replicate the full-scale one.

III. DERIVED DIMENSIONLESS PARAMETERS

As the parameters (7) and the radius a fully determine the required initial plasma state, all other characteristic dimensionless parameters can be expressed in terms of the set (7). As an example, we evaluate the product of the characteristic frequency of the large-scale drift vortices ω_D and the electron-ion energy equilibration time $\tau_{ei}^{(E)}$. We estimate the first one as

$$\omega_D = \frac{\rho_i}{a}\frac{\mathrm{v}_{Ti}}{a} \tag{13}$$

(see, e.g., [15] and references therein). The second one can be estimated as

$$\tau_{ei}^{(E)} = \lambda / \mathrm{v}_{Ti}\sqrt{\mu} \tag{14}$$

The product is the dimensionless parameter

$$\omega_D \tau_{ei}^{(E)} \equiv S_1 = \frac{1}{\sqrt{\mu} R_1 R_2} \tag{15}$$

Note that the drift frequency can be expressed in terms of the Bohm diffusion coefficient (12): using equations $\mathrm{v}_{Ti} = \sqrt{2T/m_i}$ and $\rho_i = \mathrm{v}_{Ti}/\omega_{Ci}$, one finds that $\omega_D^{-1} = a^2/(32D_B)$. In other words, ω_D^{-1} corresponds to a diffusion time over the radius a for diffusion coefficient which is more than 10 times higher than the Bohm diffusion coefficient (12). Still, the dimensionless parameter S_1 is small, meaning that the electron and ion temperature would remain equal to each other even for a very strong anomalous transport and thereby justifying the use of a single-temperature model.

Other interesting dimensionless parameter is the ratio of the resistive diffusion time over the scale a, a^2/D_M, with D_M being the magnetic diffusion coefficient, to the acoustic time (6), the magnetic Reynolds number. One has: $D_M = c^2 \nu_{ei}/\omega_{pe}^2$, where ν_{ei} is the electron-ion collision frequency, $\nu_{ei} = \mathrm{v}_{Ti}/\lambda\sqrt{\mu}$. These relations provide correct dependences of the corresponding quantities on the plasma parameters and are therefore suitable for the scaling studies; the numerical coefficients may differ by a factor of 1.5-2 from the exact values. We denote the magnetic Reynolds number as S_2. It is

$$a^2/\tau D_M \equiv S_2 = \frac{R_1^2 \beta}{2R_2\sqrt{\mu}} \tag{16}$$

The magnetic Reynolds number is very large in all cases, meaning that the magnetic diffusion is insignificant. If convection develops in a high-beta MAGLIF plasma, the

condition S_2>>1 means that the magnetic field is entrained by the plasma motion and may become tangled.

One can also express in terms of the scaling factors $R_{1\text{-}4}$ the electron magnetization, λ / ρ_e , and the ratio of the relative velocity u of the electrons and ions (the "current" velocity) to the ion thermal velocity v_{Ti}. For the scaling purposes, we use the following expressions for ρ_e and u (in CGS units):

$$\rho_e = \sqrt{\mu}\rho_i , \tag{17}$$

$$u = \left(c / 4\pi en\right) | \nabla \times B | = cB / 4\pi ena . \tag{18}$$

Using these expressions and Eqs. (2), (3), (5)-(7), we obtain:

$$\lambda / \rho_e \equiv S_3 = \frac{R_1}{R_2\sqrt{\mu}} ; \quad u / v_{Ti} \equiv S_4 = \frac{2}{\beta R_1} . \tag{19}$$

One sees that the electrons are always magnetized, S_3>>1, and that the current velocity is very small compared to the ion thermal velocity, S_4<<1, meaning that there are hardly any current-driven micro-instabilities. The parameters $S_{1\text{-}4}$ are presented in Table 3.

To evaluate the role of bremsstrahlung losses, we introduce the cooling time τ_{rad} according to definition $\dot{p} / p = -p / \tau_{rad}$. A numerical estimate of the thus defined cooling time is [18]:

$$\tau_{rad}(ns) = \frac{8.9 \times 10^{23} \sqrt{T(keV)}}{n(cm^{-3})} \tag{20}$$

The ratio of this time to the normalization time τ can be expressed as a function of the four main scaling parameters and the radius:

$$\frac{\tau_{rad}}{\tau} = \frac{1.74\times 10^5}{R_1}\sqrt{\frac{a}{\beta R_2}} \qquad (21)$$

Note that this ratio depends on a. Therefore, if we want to have this ratio to be constant between two systems, we have to make the a's the same, i.e. the scaled system would become identical to the original one, making useful scaling impossible. This is a general problem of including radiation in hydrodynamic scalings (e.g., Ref. 10). The way around is to assume that radiation is unimportant – as it must be in practical systems, i.e., the ratio (21) is large. It is indeed large in both regimes 1 and 2, Table 3.

One can show that the 2-fluid Braginski equations [17] are invariant with respect to transformations described by Eqs. (8)-(10), provided that the radiative losses are negligible. As an example, we present in Appendix the proof of scalability for the energy equation. The anomalous transport in high-beta plasma is a three-dimensional phenomenon, and this is why it is so hard to simulate it. On the other hand, the scaling approach automatically includes the three-dimensionality of the problem.

IV. EXAMPLES OF POSSIBLE SCALED EXPERIMENTS

We can now address an issue of a feasibility of scaled experiments that would allow one to address the physics issues of a full-scale experiment but would have some advantages in terms of, say, required energy and/or better diagnostic access. To identify the possible scaled experiments with the same (or close) values of the dimensionless parameters (6), we choose one dimensional parameter, the plasma radius a, that we are going to vary, and see how the other dimensional parameters change. The corresponding parameter space is illustrated by Fig. 1.

The case 1 is that of a relatively low-temperature plasma. If one holds all the dimensionless parameters constant, a 3-fold decrease of the radius (to a=1 mm) leads to the decrease of the required energy by a factor of 1.7. Other changes include a 10-fold increase of the density, ~ 4-fold increase of the magnetic field, and ~ 4-fold decrease of the time τ. These changes wouldn't make the scaled experiment on the creation and confinement of a pre-plasma much easier.

A more promising path is associated with the fact that the ions at the stage 1 are un-magnetized, $R_1 << R_2$. So, some reduction of the parameter R_1 wouldn't have any effect on the plasma confinement and would leave the plasma in the same confinement regime as for the full-scale experiment. As an example, consider the reduction of both a and R_1 by a factor of 2, leaving all other dimensionless parameters untouched. With that, the plasma energy decreases by a factor of 11, to ~ 0.6 kJ, and the magnetic field decreases by a factor of 1.6, to 0.18 MG. The density remains unchanged, the temperature decreases to ~ 200 eV and the normalization time decreases to 9 ns. The changes of that scale allow one to perform an experiment on a number of laser and pulsed-power facilities. Note that, for the plasma parameters of case 1, the change of R_1 does not lead to any significant change of the confinement regime and allows one to address the same physics as that governing the pre-plasma formation in a full-scale experiment.

Consider now a possible scaling-down of the experiment on the plasma confinement near the point of the maximum compression. Here the ions are magnetized, $R_1 >> R_2$. On the other hand, the ratio of the drift frequency for the global mode, $\omega_D = (\rho_i / a)(\mathrm{v}_{Ti} / a)$, to the ion collision frequency, $\nu_i = \mathrm{v}_{Ti} / \lambda$, is still very small,

$\omega_D / \nu_i = 1/R_1 R_2 << 1$, meaning that we are in the regime of collisional drift instabilities considered in Refs. [15, 16]. This allows considering an experiment where the parameter R_1 would be reduced by a factor of 2. The plasma is still strongly magnetized, $R_1 >> R_2$, and, at the same time, remains in the collisional drift-turbulence regime, $R_1 R_2 >> 1$. The ratio $L/\lambda = R_4 R_2$ is huge, ~ 400. This allows one to somewhat reduce the parameter R_4, say, by a modest factor of 2, so that the parallel physics would remain collision-dominated. The relative time for the axial redistribution of the plasma, $L/\tau v_{Ti} = R_4$, remains greater than 1, meaning that the plasma flow through the ends is small. The corresponding parameter domain for possible scaled experiment is shown in Fig. 1b. For the radius of a=0.25 mm which may provide more space for the plasma diagnostics, the required energy is 11 kJ, the magnetic field is 20 MG, the plasma density is 7.5×10^{21} cm^{-3}, and the plasma length is 6 mm. These parameters may be attainable in the experiment on the Omega laser facility [18] at the University of Rochester. The magnetic fields approaching 40 MG have already been reported by the Omega group [19, 20]. This has been achieved in the laser-driven cylindrical implosions with a seed magnetic field, although in smaller volumes.

The plasma parameters in these scaled experiments for the regimes mentioned above are summarized in Table 4. The rows marked as "DT" correspond to DT mixture. The rows marked by "H" correspond to the hydrogen plasma considered in the next section.

V. THE ISOTOPIC EFFECT

Thus far we have been considering the situation where the plasma in the scaled experiment would have the same composition as in a real experiment, where the average atomic mass would be 2.5. It is clear that the use of tritium in the scaled experiments will

be hardly possible, and the actual average mass for the deuterium plasma would be 2. The difference of the factor of 1.25 does not seem significant for the changes in the plasma confinement regimes and has been ignored in the present analysis. It may, however, be interesting to consider possible impact of switching to a pure hydrogen plasma, where the atomic mass would be 2.5 times less than in a fusion experiment. We therefore introduce one more dimensionless parameter into our analysis, that of the atomic weight $A=m_i/m_p$.

Only one of the 4 dimensionless parameters (6), R_1, is affected by the different atomic mass: R_1 becomes larger for the hydrogen plasma by a factor of $A^{1/2}=(2.5)^{1/2}=1.58$. Then, the dependence on the atomic weight propagates through Eqs. (8)-(11). Compared to the initial form, the following factors appear in these equations: $n\sim(A/2.5)$; $T\sim(A/2.5)^{1/2}$; $B\sim(A/2.5)^{3/4}$; $\tau\sim(A/2.5)^{1/4}$; $W\sim(A/2.5)^{3/2}$. Keeping R_1 the same as in the DT experiment would, in particular, lead to a reduction of the required energy by a factor of $(2.5)^{3/2}=4$, i.e. to ~ 150J for the first case and ~ 2.8 kJ for the second case. A summary of these changes is presented in table 4.

There may also be processes modified by the change of the atomic weight that explicitly depend on the electron mass, like the electron parallel thermal conduction and electron magnetization. On the other hand, for the set of parameters considered above both processes remain actually unaffected: the parallel heat conduction remains negligible, and the magnetization remains greater than one.

VI. DISCUSSION

The scaling analysis presented in this paper demonstrates that the properties of the MagLIF plasmas can be fully imitated in scaled-down experiments. If the four dimensionless parameters defined by Eq. (7) are held approximately the same as in a full-

size experiment, one can significantly reduce the required energy and magnetic field and still obtain experimental information pertinent to a full-size experiment. The absolute values of the plasma parameters and the time-scale do change, but the plasma behavior fully replicates the behavior of the initial experiment; such parameters as the confinement time in full-scale experiment can be found by simply changing the time scale according to Eq. (10).

Having said that, we have to emphasize that our analysis by itself does not allow one to make *predictions* of the confinement time: it describes, in a rigorous way, a *relation* between the confinement times in two systems, a large one and a much smaller one.

Interestingly, the imploded state can be emulated also in the experiment of a much larger scale, but the one that would not require multi-megagauss magnetic fields and would not involve any disposable parts. Indeed, if we assume that the plasma radius is 200 times higher than 0.12 mm of Table 1, and use hydrogen, we obtain the following set of parameters (Eqs. (8)-(11)): $n \sim 10^{18}$ cm^{-3}, $T \sim 0.35$ keV, $B \sim 5$ T, $W \sim 0.5$ MJ, $L \sim 120$ cm. Although the required plasma energy is larger, the characteristic time-scales are much longer, by a factor of $\sim 10^3$, according to Eq. (10). In other words, the heating time can be as long as 1 μs ($1000\tau^*$ of Table 1). Such plasmas can, possibly, be created by techniques used in the experiments with the E-beam heating [22] and FRC experiments [23]. A more detailed analysis of this intriguing possibility is well beyond the scope of this paper.

In summary we have shown that the scaled-down experiments can correctly reproduce the plasma state at two most critical stages of the whole implosion, the plasma formation early in the pulse, and the stage of a maximum compression. These scaled

experiments would require significantly less energy than the full-scale experiment. The goals of such experiment would be to study the process of plasma confinement and to demonstrate fulfillment of the necessary conditions for the success of the whole implosion. Importantly, scaled experiments can be performed with a variety of experimental platforms, not necessarily Z-pinch driven implosions. In particular, a number of issues can be assessed by plasma confined in a resting cylindrical shell and heated axially by a laser pulse, or heavy-ion-beam, or other technique.

Work performed for U.S. DoE by LLNL under Contract DE-AC52-07NA27344; Sandia National Laboratories is a multi-program laboratory managed and operated by Sandia Corporation, a wholly owned subsidiary of Lockheed Martin Corporation, for the U.S. DOE's NNSA under contract DE-AC04-94AL85000.

Appendix. Scalability of 2-fluid equations

We assume that the initial state of the plasma is known and is characterized by known spatial distributions of density, temperature and the magnetic field, n, T, and $\boldsymbol{B}$. The initial mass velocities are small, and we neglect them, although at later stage the flows are allowed to develop in the course of the evolution of the plasma state.

We normalize n, T, and $\boldsymbol{B}$ to their initial values in the midpoint, n_0, T_0, and B_0. The spatial coordinates are measured in the units of a, and the time in the units of τ (Eq. (6)):

$$\tilde{\boldsymbol{r}} = \boldsymbol{r} / a\,, \quad \tilde{t} = t / \tau \tag{A1}$$

The parameters $R_{1\text{-}4}$ and τ are constructed from n_0, T_0, B_0, a and L.

The normalized equations are formulated in terms of functions $\tilde{n}(\tilde{\boldsymbol{r}},\tilde{t})$, $\tilde{T}(\tilde{\boldsymbol{r}},\tilde{t})$ and $\tilde{\boldsymbol{B}}(\tilde{\boldsymbol{r}},\tilde{t})$ related to the initial functions by

$$n(\boldsymbol{r},t) = n_0\tilde{n}(\tilde{\boldsymbol{r}},\tilde{t})\,,\; T(\boldsymbol{r},t) = T_0\tilde{n}(\tilde{\boldsymbol{r}},\tilde{t})\,,\; \boldsymbol{B}(\boldsymbol{r},t) = B_0\tilde{\boldsymbol{B}}(\tilde{\boldsymbol{r}},\tilde{t}) \tag{A2}$$

The flow velocity $\mathbf{v}(\boldsymbol{r},t)$ that appears in the course of plasma evolution is normalized as

$$\mathbf{v}(\boldsymbol{r},t) = \frac{a}{\tau}\tilde{\mathbf{v}}(\tilde{\boldsymbol{r}},\tilde{t}) \tag{A3}$$

For the case of a rapid electron-ion energy exchange, one can sum-up the electron and ion energy equations (2.3e) and (2.3i) of Ref. 17 to obtain:

$$3n\left(\frac{\partial T}{\partial t} + \mathbf{v}\cdot\nabla T\right) + 2nT = -\nabla\cdot\boldsymbol{q} - \pi_{\alpha\beta}\frac{\partial \mathrm{v}_\alpha}{\partial x_\beta} + Q_e + Q_i \tag{A4}$$

where $\boldsymbol{q}$ is the heat flux, $\pi_{\alpha\beta}$ is a viscous stresses tensor, and Q is the heating power per unit volume, other than viscous heating described by the second term in the r.h.s. We focus here on the heat flux driven by the temperature gradient; the other terms which we

denote further by … can be treated identically. The expression for the temperature-driven heat flux is

$$q_\alpha = -\kappa_{\alpha\beta}\frac{\partial T}{\partial x_\beta} \tag{A5}$$

The general structure of the heat conductivity tensor is [17]:

$$\kappa_{\alpha\beta} = n\mathrm{v}_{Ti}\lambda f_{\alpha\beta}(\mu, \rho_i/\lambda) \tag{A6}$$

where $f_{\alpha\beta}$ are dimensionless functions. [In specific analyses, this expression is used in the form $\boldsymbol{q} = -\kappa_{\|}\nabla_{\|}T - \kappa_{\perp}\nabla_{\perp}T - \kappa_{\wedge}\boldsymbol{b}\times\nabla T$.]

By switching to new variables, we have:

$$3\tilde{n}\left(\frac{\partial\tilde{T}}{\partial\tilde{t}} + \tilde{\mathbf{v}}\cdot\tilde{\nabla}\tilde{T}\right) + 2\tilde{n}\tilde{T}\tilde{\nabla}\tilde{\mathbf{v}} = -\frac{1}{R_2}\tilde{\nabla}\cdot(g_{\alpha\beta}\tilde{\nabla}\tilde{T}) + \ldots$$

where

$$g_{\alpha\beta} = \tilde{T}^{5/2} f_{\alpha\beta}(\mu, \frac{R_2}{R_1}\frac{\tilde{n}}{\tilde{B}\tilde{T}^{3/2}}) \tag{A7}$$

One sees that the two systems characterized by the same dimensionless scaling parameters are described by the same equations and are therefore indistinguishable in their behavior, up to the scaling transformations. We have shown this for one of the of equations, but one can check that the whole set of Ref. [17] maintains these invariance properties.

References.

1. S. A. Slutz, M. C. Herrmann, R. A. Vesey, A. B. Sefkow, D. B. Sinars, D. C. Rovang K. J. Peterson, and M. E. Cuneo. "Pulsed-power-driven cylindrical liner implosions of laser preheated fuel magnetized with an axial field." Phys. Plasmas, **17**, 05603 (2010).
2. M. Shimada, D.J. Campbell, V. Mukhovatov, et al. "Progress in the ITER Physics Basis: Overview and Summary." Nucl. Fusion, **47**, S1 (2007).
3. J. D. Lindl. "Development of the indirect-drive approach to inertial confinement fusion and the target physics basis for ignition and gain." Phys. Plasmas, **2**, 3933 (1995).
4. M.K. Matzen, B.W. Atherton, M.E. Cuneo, et al. "The Refurbished Z facility: Capabilities and Recent Experiments", Acta Physica Polonica, **A115**, 956 (2009).
5. R.C. Kirkpatrick, I.R. Lindemuth, M.S. Ward. "Magnetized Target Fusion: an Overview." Fusion Technology," **27**, 201 (1995).
6. R.P. Drake, J. Hammer, C. Hartman, et al. "Submegajoule liner implosion of a closed field line configuration". Fusion Technology, **30**, 310 (1996).
7. R.E. Siemon, I.R. Lindemuth, K.F. Schoenberg. "Why Magnetized Target Fusion Offers a Low-Cost Development Path for Fusion Energy." *Comments on Plasma Physics and Controlled Fusion*, **18**, 363 (1999).
8. G.A. Wurden, T.P. Intrator, P.E. Sieck, "FRCHX Magnetized Target Fusion HEDLP Experiments." Paper IC/P4-13, *Proc. 2008 Fusion Energy Conference*, IAEA, Vienna, 2008, (http://www-pub.iaea.org/MTCD/Meetings/fec2008pp.asp)

9. D.D. Ryutov, R. P. Drake, J. Kane, et al. "Similarity criteria for the laboratory simulation of supernova hydrodynamics." Astrophysical Journal, **518**, 821 (1999).
10. D.D. Ryutov, B.A. Remington, H.F. Robey, R.P. Drake. "Magnetohydrodynamic scaling: from astrophysics to the laboratory," Phys. Plasmas, **8**, 1804 (2001).
11. S.A. Slutz, M.R. Douglas, J.S. Lash, et al. "Scaling and optimization of the radiation temperature in dynamic hohlraums." Phys. Plasmas, **8**, 1673 (2001).
12. D.B. Sinars, S.A. Slutz, M.C. Herrmann et al. "Measurements of Magneto-Rayleigh-Taylor Instability Growth during the Implosion of Initially Solid Al Tubes Driven by the 20-MA, 100-ns Z Facility." Phys. Rev. Lett., **105**, 185001 (2010).
13. D.B. Sinars, S.A. Slutz, M.C. Herrmann et al. "Measurements of magneto-Rayleigh-Taylor instability growth during the implosion of initially solid metal liners." Phys. Plasmas, **18**, 056301 (2011).
14. A. ElNadi, M.N. Rosenbluth. "Infinite-beta limit of drift instability." Phys. Fluids, **16**, 2036 (1973).
15. D.D. Ryutov. "On Drift Instabilities in Magnetized Target Fusion Devices." Physics of Plasmas, **9**, 4085 (2002).
16. D.D. Ryutov, D. Barnes, B. Bauer, et al. "Particle and heat transport in a dense wall-confined MTF plasma (theory and simulations)". "Nuclear Fusion," **43**, 955, (2003).
17. S.I. Braginski, "Transport Processes in a Plasma," In: Reviews of Plasma Physics, M.A. Leontovich, Ed. Consultants Bureau, New York, 1965.
18. D.L.Book. "NRL Plasma Formulary." Naval Research Laboratory (1987).

19. T.R. Boehly, R. L. McCrory, C. P. Verdon, et al. "Inertial confinement fusion experiments with OMEGA-A 30-kJ, 60-beam UV laser," Fusion Eng. Des. 44, 35 (1999).

20. J. P. Knauer, O.V. Gotchev, P. Y. Chang, et al., "Compressing magnetic fileds with high-energy lasers." Phys. of Plasmas, **17**, 056318 (2010).

21. P.Y. Chang, G. Fiksel, M. Hohenberger et al. "Fusion yield enhancement in magnetized laser-driven implosions," Phys. Rev. Lett., **107**, 035006 (2011).

22. A. V. Burdakov, A. V. Arzhannikov, V. T. Astrelin et al. "Concept of fusion reactor based on multiple-mirror trap, Fusion Sci. and Techn." **59**, 307 (2011).

23. T. P. Intrator, G.A. Wurden, W.J. Waganaar et al. "Design and features of the magnetized target fusion experiment." *Current Trends in International Fusion Research*, AIP Conference Proceedings, v. 1154, p. 65 (2009).

Table 1. Characteristic plasma parameters for 3 stages of the implosion: right after creating the pre-plasma (1) and at the maximum compression (2). The last 4 columns represent parameters evaluated by Eqs. (2)-(4).

	n, 10^{21}cm^{-3}	T(keV)	B(MG)	a(mm)	L(mm)	τ*(ns)	τ(ns)	ρ_i(μm)	λ(μm)	W(kJ)
1	0.3	0.3	0.3	3	6	20	18	142	9	7.3
2	120	8	130	0.12	6	2	0.14	1.7	16	124

Table 2. Scaling parameters (6) for the two phases of the pinch implosion

	$R_1 = \frac{a}{\rho_i}$	$R_2 = \frac{a}{\lambda}$	$R_3 = \beta$	$R_4 = \frac{L}{a}$
1	21	330	80	2
2	70	7.5	4.6	50

Table 3. Secondary dimensionless parameters for the two phases of pinch implosion*

	S_1	S_2	S_3	S_4	τ_{rad}/τ
1	10^{-3}	3.6×10^{3}	4.3	1.2×10^{-3}	88
2	0.13	10^{5}	634	6.2×10^{-3}	146

*S_1 is the ratio of the drift time to the electron-ion energy equilibration time (Eq.15)); S_2 is the magnetic Reynolds number (Eq. (16)); S_3 is the electron magnetization parameter (Eq. (19)); S_4 is the ratio of the "current" velocity to the ion thermal velocity (Eq. (19)).

Table 4. Parameters of the scaled-down experiments

		a(mm)	R_1	R_2	R_3	R_4	n, 10^{21}cm^{-3}	T(keV)	B(MG)	$W(kJ)$	τ(ns)	τ_{rad}/τ
1	DT	1.5	10.5	330	80	2	0.3	0.2	0.18	0.6	6	130
	H	1.5	10.5	330	80	2	0.12	0.13	0.09	0.15	4.8	325
2	DT	0.25	35	7.5	4.6	25	7.5	3	20	11	0.25	460
	H	0.25	35	7.5	4.6	25	3	1.9	10	2.7	0.2	1150

Figure caption

Fig. 1. The parameter domain for MAGLIF simulation experiments. (a) An early part of the implosion; the dimensionless parameters are taken from the first row of Table 2; (b) A plasma near the point of the maximum compression. The dimensionless parameters are those of the second row of Table 2, except for R_1 and R_4, which are 35 and 25, respectively.

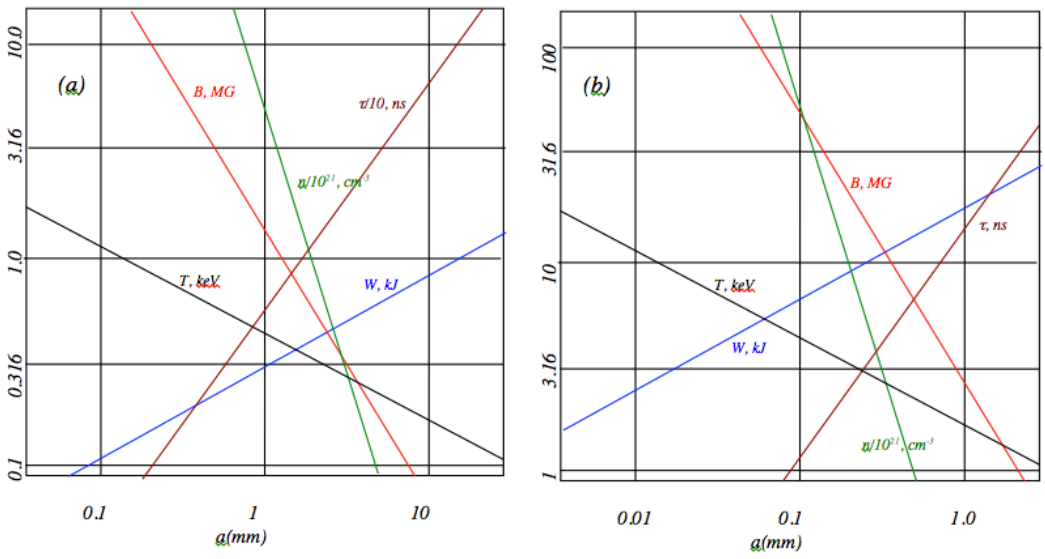
(a)
B, MG
τ/10, ns
η/10^21, cm^-3
T, keV
W, kJ
10.0
3.16
1.0
0.316
0.1
0.1
1
10
a(mm)
(b)
B, MG
τ, ns
T, keV
W, kJ
η/10^21, cm^-3
100
31.6
10
3.16
1
0.01
0.1
1.0
a(mm)

Fig. 1